34th Annual International Conference of the IEEE EMBS
San Diego, California USA, 28 August - 1 September, 2012

Granger Causality in Cardiovascular Variability Series: Comparison between Model-based and Model-free Approaches

Alberto Porta, *Member, IEEE*, Tito Bassani, Vlasta Bari, Stefano Guzzetti

***Abstract*—A linear model-based (MB) approach for the evaluation of Granger causality is compared to a nonlinear model-free (MF) one. The MB method is based on the identification of the coefficients of a multivariate linear regression via least-squares procedure. The MF technique is grounded on the concept of local prediction and exploits the k-nearest-neighbors approach. Both the methods optimize the multivariate embedding dimension but MF technique is more parsimonious since the number of components taken from each signal can be different. Both methods were applied to the variability series of heart period (HP), systolic arterial pressure (SAP) and respiration (R) recorded during spontaneous and controlled respiration at 15 breaths/minute (SR and RC15) in 19 healthy humans. Both MB and MF methods revealed the increase of HP predictability during RC15 and the unmodified causality from SAP to HP and from R to HP during RC15, thus suggesting that nonlinear methods are not superior to the linear ones in assessing predictability and causality in healthy humans.**

I. Introduction

CAUSALITY provides indication about the mechanisms involved in cardiovascular control. For example, causality analysis suggested that in healthy humans at rest the dominant causal direction of interactions is from heart period (HP) to systolic arterial pressure (SAP) as a result of Starling law and diastolic runoff, while the decrease of the venous return induced by the orthostatic stimulus leads to the prevalence of the reverse causal direction [1].

The operative definition of causality given by Granger in the field of multivariate stochastic processes provided a viable framework to assess causality in time series [2]. Given a set of M signals, Ω, describing the behavior of the system under study, the time series y_j Granger-causes another time series y_i in Ω if y_i can be predicted better in Ω than in Ω after excluding y_j. In other words, y_j Granger-causes y_i in Ω if y_j carries an unique information about the future evolution of y_i that cannot be derived from any other signal present in Ω.

Granger causality is traditionally estimated based on the description of the interactions among signals according to a multivariate linear regression model [3]. However, this model-based (MB) approach is adequate only when the interactions among signals are linear. Conversely, if dynamics are nonlinear, this approach might fail in interpreting dynamical interactions among processes, thus resulting in an erroneous interpretation of causal relations.

Local prediction approach provides a multivariate framework for evaluating predictability of a process by relaxing the hypothesis of linear interactions [4]. Local prediction approach assumes that two samples of the same signal (i.e. $y_i(k)$ and $y_i(j)$) will be close if the embedding vectors $Z_i(k)=(y_1(k),\ldots, y_1(k-p),\ldots, y_i(k-1),\ldots, y_i(k-p),\ldots, y_M(k),\ldots, y_M(k-p))$ and $Z_i(j)=(y_1(j),\ldots, y_1(j-p),\ldots, y_i(j-1),\ldots, y_i(j-p),\ldots, y_M(j),\ldots, y_M(j-p))$ formed by present and past samples of the signals belonging to Ω are similar, thus forecasting the future based on the knowledge of the past. Since this approach does not impose any form to the function mapping embedding vectors into y_i, nonlinearities, if present, can be described via a model-free (MF) method.

The aim of this study is to compare the traditional linear MB approach to the assessment of Granger causality with a nonlinear MF method based on local prediction. The issue of the reconstruction of the multivariate embedding space and optimization of the multivariate embedding dimension will be considered in both approaches. The two approaches will be tested over cardiovascular beat-to-beat variability of HP, SAP and respiration (R) during an experimental maneuver known to increase the likelihood to observe nonlinear HP dynamics (i.e. paced breathing) [5-7]. Indexes assessing causality from R to HP due to the direct influences of respiratory centers on vagal efferent activity and, in turn, on HP, and from SAP to HP due to cardiac baroreflex control will be estimated.

II. Methods

A. General Definitions

Given M series $y_1=\{y_1(k), k=1,...,N\},\ldots, y_M=\{y_M(k), k=1,...,N\}$ where N is the series length and k is the progressive counter, they are first normalized to have zero mean and unit variance. We define $\Omega=\{y_1,\ldots,y_i,\ldots,y_j,\ldots,y_M\}$ as the universe of our knowledge about the system under study. After labeling $Y_j^i(k)=(y_j(k-\tau_j^i),\ldots, y_j(k-p))$ the embedding vector formed by $p_j^i=p-\tau_j^i+1$ components of y_j, where τ_j^i represents the delay of the influence of y_j on y_i, the

Manuscript received March 15, 2012. This work was supported in part by the Telethon GGP09247 grant to A. Porta.

A. Porta and T. Bassani are with the Department of Biomedical Sciences for Health, Galeazzi Orthopedic Institute, University of Milan, Milan, Italy (tel: +39 02 50319976; fax: +39 02 50319960; e-mails: alberto.porta@unimi.it and tito.bassani@libero.it).

V. Bari is with the Department of Bioengineering, Politecnico di Milano, and the Department of Biomedical Sciences for Health, Galeazzi Orthopedic Institute, University of Milan, Milan, Italy (e-mail: vlasta.bari@gmail.com).

S. Guzzetti is with the Department of Emergency, L. Sacco Hospital, Milan, Italy (e-mail: guzzetti.stefano@hsacco.it).

multivariate embedding vector accounting for all signals present in Ω is $Z_i(k)=(Y_1^i(k),\ldots,Y_i^i(k),\ldots,Y_j^i(k),\ldots,Y_M^i(k))$ and has dimension

$$q_i = M \cdot (p+1) - \sum_{k=1}^{M} \tau_k^i \qquad (1)$$

where $1\le\tau_i^i\le p$ and $0\le\tau_k^i\le p$ with $1\le k\le M$ and $k\neq i$. All the multivariate embedding vectors form a set $Z_i=\{Z_i(k), k=p+1,...,N\}$. We model y_i in Ω as

$$y_i(k) = f(Z_i(k)) + \varepsilon_i(k) \qquad (2)$$

where $f(\cdot)$ represents the predicable portion of y_i based on Z_i and ε_i is the unpredictable part modeled as a white noise with zero mean and variance λ_i^2.

These definitions can be easily extended to the universe Ω after the exclusion of y_j, i.e. $\Omega/y_j=\{y_1,\ldots,y_i,\ldots,y_M\}$. In this case the multivariate embedding vector obtained from $Z_i(k)$ after excluding $Y_j^i(k)$ is $Z_i(k)/Y_j^i(k)=(Y_1^i(k),\ldots, Y_i^i(k),\ldots, Y_M^i(k))$ and the set of $Z_i(k)/Y_j^i(k)$ is indicated as Z_i/Y_j^i.

B. Linear MB Approach

In the linear MB approach $f(\cdot)$ is a linear combination of the components of $Z_i(k)$ [3]. Traditional least-squares procedure can be exploited to estimate the coefficients of the linear combination minimizing the variance of ε_i. After the optimization procedure the variance of the prediction error $\hat{\lambda}_i^2$ can be evaluated. Due to normalization, $\hat{\lambda}_i^2$ ranges between 0 and 1, indicating full and null predictability of y_i respectively. $\hat{\lambda}_i^2$ is a function of the multivariate embedding dimension, q_i. Since in linear MB approach it is a common practice to build progressively the multivariate embedding space by adding a delayed component for each signal (i.e. M components at a time), $\hat{\lambda}_i^2$ finally depends only on p [3] and p is usually referred to as the model order. It is well-known that $\hat{\lambda}_i^2$ decreases towards 0 with p when $\hat{\lambda}_i^2$ is assessed "in-sample" (i.e. $\hat{\lambda}_i^2$ is assessed over the same set of data utilized to estimate the coefficients of the multivariate linear regression). Therefore, cost functions are usually exploited to penalize large p. These cost functions are combined with $\hat{\lambda}_i^2$ leading to figures of merit (e.g. Akaike figure of merit [8]) the minimum of which allows the optimization of p and, in turn, the optimization of the multivariate embedding dimension, q_i. Defined as p^o the model order minimizing the selected figure of merit, thus leading to an optimal multivariate embedding dimension, q_i^o, we indicate with $\hat{\lambda}_i^2(Z_i^{q_i^o})$ the variance of the prediction error at q_i^o. The MB goodness of fit of y_i ($MBGF_i$) is computed as the variance of the predictable part (i.e. $1-\hat{\lambda}_i^2(Z_i^{q_i^o})$ due to normalization).

C. Linear MB Granger Causality Approach

The linear MB Granger causality from y_j to y_i is assessed according to the MB causality ratio ($MBCR_{ij}$)

$$MBCR_{ij} = \frac{\hat{\lambda}_i^2(Z_i^{q_i^{jo}}/Y_j^i) - \hat{\lambda}_i^2(Z_i^{q_i^o})}{\hat{\lambda}_i^2(Z_i^{q_i^o})} \qquad (3)$$

where $\hat{\lambda}_i^2(Z_i^{q_i^{jo}}/Y_j^i)$ and $\hat{\lambda}_i^2(Z_i^{q_i^o})$ represent the variance of the prediction error assessed at the optimal multivariate embedding dimension in Ω/y_j and Ω (i.e. q_i^{jo} and q_i^o) respectively. $MBCR_{ij}$ quantifies the worsening of the prediction of y_i when y_j is excluded from Ω. If $\hat{\lambda}_i^2(Z_i^{q_i^{jo}}/Y_j^i)$ is significantly larger than $\hat{\lambda}_i^2(Z_i^{q_i^o})$, then y_j Granger-causes y_i in Ω [2].

D. Nonlinear MF Approach

K-nearest-neighbors approach can be exploited to perform local prediction [4]. The k-nearest-neighbors approach calculates the best prediction of $y_i(k)$ in Ω as a combination (usually the weighted mean [9]) over a subset of values of y_i whose associated multivariate embedding vectors belong to the set of the k nearest neighbors of $Z_i(k)$. The closeness of points to $Z_i(k)$ is decided according to a predefined norm (usually the Euclidean norm). After calculating the prediction of y_i in Ω the square correlation coefficient between y_i and its prediction, r_i^2, can be assessed [9]. r_i^2 is bounded between 0 and 1 indicating null predictability and perfect predictability of y_i. We followed a different strategy to build progressively the multivariate embedding space with respect to that utilized in the MB approach. Instead of adding one delayed component from each signal belonging to Ω at a time (i.e. M components at a time) as in the MB method, we added only one delayed sample at a time. Initially, the set of candidate new samples was $\{y_1(k-\tau_1^i),\ldots, y_1(k-P), \ldots, y_M(k-\tau_M^i),\ldots, y_M(k-P)\}$ where P is the maximum delay of the influences of each signal on y_i. The added new sample was taken from the set of candidates as the one optimizing a criterion [10,11], i.e. here the maximization of r_i^2 at a given q_i. As q_i was increased, the set of candidates was reduced by excluding samples of a signal with time indexes more recent or equal to any component of the same signal already utilized to form the multivariate embedding space, thus avoiding duplicate selections and speeding up reconstruction. r_i^2 varies with q_i. If Z_i is helpful to predict y_i, r_i^2 exhibits a maximum over q_i [9]. Indeed, when q_i is low, the dynamics of y_i is roughly predicted and, when q_i is high, the prediction worsens due to the scattering of points in the multivariate embedding space making the k nearest neighbors too far away to reliably predict future behaviors. Defined as q_i^o the optimal multivariate embedding dimension, we indicate with $r_i^2(Z_i^{q_i^o})$ the square correlation coefficient between y_i and its prediction at q_i^o. The MF goodness of fit of y_i ($MFGF_i$) is computed as $r_i^2(Z_i^{q_i^o})$.

E. Nonlinear MF Granger Causality Approach

The nonlinear MF Granger causality from y_j to y_i is assessed according to the MF causality ratio ($MFCR_{ij}$)

$$MFCR_{ij} = \frac{r_i^2(Z_i^{q_i^o}) - r_i^2(Z_i^{q_i^{jo}} / Y_j^i)}{r_i^2(Z_i^{q_i^{jo}} / Y_j^i)} \quad (4)$$

where $r_i^2(Z_i^{q_i^o})$ and $r_i^2(Z_i^{q_i^{jo}} / Y_j^i)$ represent the square correlation coefficient assessed at the optimal multivariate embedding dimension in Ω and Ω/y_j respectively (i.e. q_i^o and q_i^{jo}). $MFCR_{ij}$ quantifies the improvement of the correlation between y_i and its prediction when y_j is included in Ω/y_j. According to the framework of the Granger causality [2], if $r_i^2(Z_i^{q_i^o})$ is significantly larger than $r_i^2(Z_i^{q_i^{jo}} / Y_j^i)$, then y_j Granger-causes y_i in Ω.

III. Experimental Protocol and Data Analysis

A. Experimental Protocol

We studied 19 healthy humans (aged from 27 to 35, median=31; 11 females and 8 males). ECG (lead II), noninvasive arterial pressure (Finapres 2300, Ohmeda, Englewood, CO, USA) and respiratory flow via a nasal thermistor (Marazza, Monza, Italy) were recorded. Signals were sampled at 300 Hz. The experimental protocol included two sessions at rest in supine position: during spontaneous respiration (SR) and during controlled respiration at 15 breaths/minute (RC15). During RC15 the subject breathed according to a metronome. All the sessions lasted 10 minutes. The protocol adhered to the principles of the Declaration of Helsinki and was approved by ethical review board of the "L. Sacco" Hospital.

B. Series Extraction

After detecting the QRS complex on the ECG and locating its apex using parabolic interpolation, HP was approximated as the temporal distance between two consecutive QRS peaks on the ECG. The i-th SAP was taken as the maximum arterial pressure value inside the i-th HP. The i-th respiratory sample was taken at the first QRS peak delimiting the i-th HP. The length of the HP, SAP and R series was N=256. Series were linearly detrended.

C. Assessment of Causality in Experimental Data

Defined as y_1=hp, y_2=sap and y_3=r we calculated $MBGF_1$ and $MFGF_1$ in $\Omega=\{y_1,y_2,y_3\}$ and $MBCR_{12}$, $MFCR_{12}$, $MBCR_{13}$ and $MFCR_{13}$. We set $\tau_2^1=0$ and $\tau_3^1=0$ to describe the fast vagal reflex (within the same cardiac beat) capable to modify HP in response to changes of SAP and R [12,13]. The coefficients of the MB approach were identified using least-squares procedure and Cholesky decomposition method [3]. Akaike figure of merit was utilized to optimize the model order, p, in the range from 4 to 16 [8]. In the MF approach k was equal to 30, the maximum value for p and q_1, P and Q_1, was 10 and 12 respectively. In both MB and MF methods q_i^{jo} was computed as q_i^o minus the optimal number of components relevant to y_j assessed in Ω.

D. Statistical Analysis

Paired t-test was utilized to check differences between parameters during SR and RC15. If the normality test (Kolmogorov-Smirnov test) was not fulfilled, Wilcoxon signed rank test was utilized. After pooling together parameters relevant to SR and RC15 the same test was utilized to assess differences between MB and MF approaches. A $p<0.05$ was considered as significant.

IV. Results

During SR the respiratory rate was 0.25±0.03 Hz and it was insignificantly different from that during RC15.

Figure 1 shows the box-and-whiskers plots reporting the 10th, 25th, 50th, 75th and 90th percentiles of $MBGF_1$ (Fig.1a) and $MFGF_1$ (Fig.1b), Both MB and MF approaches suggested that predictability of y_1 increased during RC15. When data relevant to SR and RC15 conditions were pooled together, $MBGF_1$ was significantly larger than $MFGF_1$.

Figure 2 shows the box-and-whiskers plots reporting the 10th, 25th, 50th, 75th and 90th percentiles of indexes assessing causality from y_2 to y_1, i.e. $MBCR_{12}$ (Fig.2a) and $MFCR_{12}$ (Fig.2b), and from y_3 to y_1, i.e. $MBCR_{13}$ (Fig.2c) and $MFCR_{13}$ (Fig.2d). Independently of the method utilized to assess predictability, causality indexes during RC15 were similar to those during SR. When data relevant to SR and RC15 conditions were pooled together, $MBCR_{12}$ was significantly larger than $MFCR_{12}$, while $MBCR_{13}$ and $MFCR_{13}$ were similar.

V. Discussion

To the best of our knowledge this is the first study comparing causality indexes evaluated according to a linear MB approach with those derived from a nonlinear MF one. MB method is based on the estimation of the coefficients of a multivariate linear regression through traditional least-squares procedure, on a strategy building progressively the multivariate embedding space by adding a component from each signal, and on the optimization of the multivariate embedding dimension through the Akaike figure of merit. MF technique is based on the local prediction paradigm and on the k-nearest-neighbors approach, on a strategy building

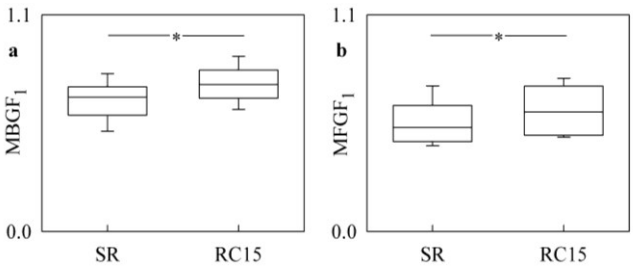

Fig.1. Box-and-whiskers plots report 10th, 25th, 50th, 75th and 90th percentiles of $MBGF_1$ (a) and $MFGF_1$ (b) during SR and RC15.

progressively the multivariate embedding space by selecting inside the overall set of delayed samples that component maximizing the square correlation coefficient between signal and its prediction at a given multivariate embedding dimension, and on the optimization of the multivariate embedding dimension according to a procedure maximizing the agreement between the signal and its prediction in the multivariate embedding space.

Independently of the technique utilized to make prediction HP series is more predictable in Ω during RC15 than during SR (Fig.1). This loss of complexity of the HP dynamics might be the effect of the regularization of the respiratory sinus arrhythmia and of slower HP rhythms imposed by paced breathing. It is worth stressing that a tendency towards a decreased complexity during RC15 has been already observed based on monovariate analysis of HP dynamics [9]. The multivariate analysis proposed in this study makes this finding significant. At first sight prediction based on the MF approach might appear to be less accurate than that of the MB method (i.e. the goodness of fit is lower). However, this finding is simply the result of the significantly smaller number of delayed samples utilized to make the MF prediction compared to the MB one. Indeed, the proposed strategy to build the multivariate embedding space in the MF approach constructs the conditioning pattern using only those components actually helpful to improve prediction.

MB and MF approaches are equivalent in assessing indexes of causality (Fig.2). Since HP dynamics exhibit nonlinear components during RC15 [9], we suggest that these nonlinearities do not affect significantly the estimate of causality indexes. Future studies should apply surrogate data analysis [14] to clarify whether the relation from SAP to HP or from R to HP (or both) is responsible for nonlinear components of the HP dynamics.

VI. Conclusion

Findings of this study indicate that a nonlinear MF method based on k-nearest-neighbors approach is not superior to the linear MB one in assessing predictability and causality in cardiovascular variability series recorded from healthy subjects. Since nonlinearities are present in the HP series, especially during paced breathing, we suggest that nonlinear components are weak and well approximated by a linear model, thus limiting the advantage of using a nonlinear approach, such as the MF one. In pathological population, where the contribution of nonlinearities is more evident, the advantage of using a MF technique might become manifest and the proposed MF technique might become a tool to quantify more consistently than linear MB approaches [15] causality in the cardiovascular control.

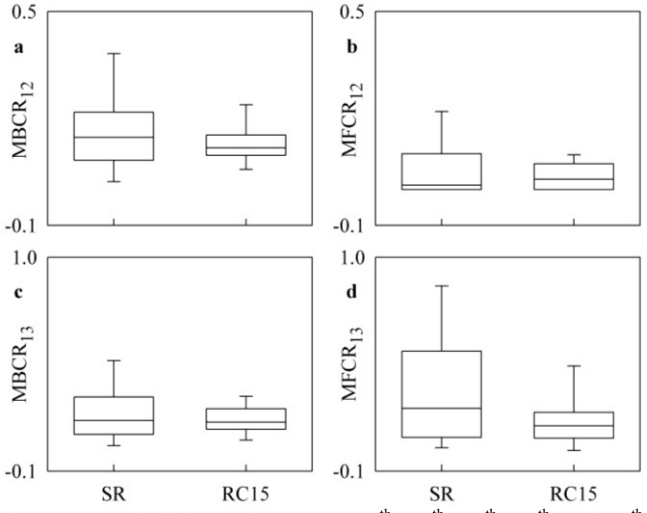

Fig.2. Box-and-whiskers plots report 10th, 25th, 50th, 75th and 90th percentiles of $MBCR_{12}$ (a), $MFCR_{12}$ (b), $MBCR_{13}$ (c) and $MFCR_{13}$ (d) during SR and RC15.

Acknowledgment

Telethon Grant GGP09247 to A. Porta partially supported the study.

References

[1] A. Porta, A.M. Catai, A.C.M. Takahashi, V. Magagnin, T. Bassani, E. Tobaldini, P. van de Borne, N. Montano, "Causal relationships between heart period and systolic arterial pressure during graded head-up tilt," *Am J Physiol*, vol. 300, pp. R378-R386, 2011.

[2] C. W. J. Granger, "Testing for causality. A personal viewpoint," J. *Econ. Dyn. Control*, vol. 2, pp. 329-352, 1980.

[3] T. Soderstrom and P. Stoica, System identification. Englewood Cliffs, NJ: Prentice Hall, 1988.

[4] H.D.I. Abarbanel, T.A: Carroll, L.M. Pecora, J.J. Sidorowich, L.S. Tsimring, "Predicting physical variables in time-delay embedding," *Phys Rev E* vol. 49, 1840-1853, 1994.

[5] K. Kanters, M.V. Hojgaard, E. Agner, and N.-H. Holstein-Rathlou, "Influence of forced respiration on nonlinear dynamics in heart rate variability," *Am J Physiol*, vol. 272, pp. R1149-R1154, 1997.

[6] J.-O. Fortrat, Y. Yamamoto, and R.L. Hughson, "Respiratory influences on non-linear dynamics of heart rate variability in humans," *Biol Cybern*, vol. 77, pp. 1-10, 1997.

[7] A. Porta, G. Baselli, S. Guzzetti, M. Pagani, A. Malliani, S. Cerutti, "Prediction of short cardiovascular variability signals based on conditional distribution," *IEEE Trans Biomed Eng*, vol. 47, pp. 1555-1564, 2000.

[8] H. Akaike, "A new look at the statistical novel identification," *IEEE Trans. Autom. Contr.*, vol. 19, pp. 716-723, 1974.

[9] A. Porta, S. Guzzetti, R. Furlan, T. Gnecchi-Ruscone, N. Montano, A. Malliani, "Complexity and nonlinearity in short-term heart period variability: comparison of methods based on local nonlinear prediction," *IEEE Trans Biomed Eng*, vol. 54, pp. 94-106, 2007.

[10] L. Faes, G. Nollo, A. Porta, "Information-based detection of nonlinear Granger causality in multivariate processes via a nonuniform embedding technique," *Phys Rev E*, vol. 83, 051112, 2011.

[11] I. Vlachos, D. Kugiumtzis, "Nonuniform state-space reconstruction and coupling detection," *Phys Rev E*, vol. 82, 016207, 2010.

[12] A. Porta, G. Baselli, O. Rimoldi, A. Malliani, M. Pagani, "Assessing baroreflex gain from spontaneous variability in conscious dogs: role of causality and respiration," *Am J Physiol*, vol. 279, pp. H2558-H2567, 2000.

[13] D. L. Eckberg, "Temporal response patterns of the human sinus node to brief carotid baroreceptor stimuli," *J. Physiol.*, vol. 258, pp. 769-782, 1976.

[14] D. Prichard and J. Theiler, "Generating surrogate data from time series with several simultaneously variables," *Phys Rev Lett*, vol. 73, pp. 951-954, 1994.

[15] A. Porta, T. Bassani, V. Bari, G.D. Pinna, R. Maestri, S. Guzzetti, "Accounting for respiration is necessary to reliably infer Granger causality from cardiovascular variability series," *IEEE Trans Biomed Eng*, vol. 59, pp. 832-841, 2012.